ECCOMAS Congress 2016
VII European Congress on Computational Methods in Applied Sciences and Engineering
M. Papadrakakis, V. Papadopoulos, G. Stefanou, V. Plevris (eds.)
Crete Island, Greece, 5–10 June 2016

# RELATIVE ROLES OF MECHANICS AND BIOCHEMISTRY IN THE INITIATION AND PROGRESSION OF CEREBRAL ANEURYSM THROMBOSIS

**Malebogo N. Ngoepe[1,2], and Yiannis Ventikos[3]**

[1] Department of Mechanical Engineering
University of Cape Town, Cape Town, South Africa
malebogo.ngoepe@uct.ac.za

[2] Centre for High Performance Computing
CSIR, Cape Town, South Africa
malebogo.ngoepe@uct.ac.za

[3] Department of Mechanical Engineering
University College London, London, United Kingdom
y.ventikos@ucl.ac.za

**Keywords:** thrombosis, computational fluid dynamics, biochemistry, cerebral aneurysms

**Abstract.** Clotting in cerebral aneurysms can either serve to stabilise an aneurysm, or can accelerate the time to rupture. In the former case, it is thought that a fully occlusive clot is likely to reduce complex haemodynamic conditions within the aneurysm sac, thereby reducing the chances of rupture. In cases where the clot fills the aneurysm sac partially, further vascular wall degradation has been observed, thus accelerating the time to rupture. The aim of this study is to determine the relative contributions of mechanical processes and biochemistry in the process of cerebral aneurysm clot development. An idealised model of an aneurysm was developed and used as the geometry of interest. This made it possible to make comparisons without a strong dependence on the peculiarities of a specific patient's case. The CFD-ACE+ Multiphysics Package (ESI Group, Paris, France) was used to calculate flow and account for the transport and reaction of biochemical species that contribute to the clotting process. In addition, user-defined functions were used to write a code that coupled the flow, biochemistry and level-set methods, which made it possible to track the surface of the growing clot, and distinguish between normal and clotted blood. The model was then used to examine the relative contributions of mechanics and biochemistry to the initiation and progression of clotting. It was found that the process of clot initiation is governed mainly by mechanical processes. Biochemistry plays a greater role in the progression of the clot where thrombin, the key player in thrombosis contributes to the formation of fibrin and thus, to the stability of the clot.

## 1 INTRODUCTION

Thrombosis is a condition that is often observed in cerebral aneurysms [1]. In some instances, the presence of a clot can advance vascular wall degradation and thereby accelerate the processes that lead to rupture [2]. In other cases, the presence of a clot in the aneurysm can lead to a more stable situation [3]. Owing to the highly patient-specific nature of aneurysms and of coagulation, it has proven rather challenging to fully identify the factors that make one clot desirable and another not. What has been observed is that a fully occlusive clot in the sac tends to prevent complex flow conditions that are often thought to be a high risk factor for rupture [4], [5]. An additional layer of complexity is introduced by the observation of both spontaneous and device-induced thrombosis in aneurysms [6]–[8]. In order to understand how best to treat cerebral aneurysms, it is necessary that steps be taken in an effort to better understanding clotting in cerebral aneurysms. A key aspect to deciphering clotting is exploring the contributions of mechanics and biochemistry to the process.

Given the elusive timing of clot formation and general difficulty of observing the role of the various miniscule components that make up the coagulation system *in vivo*, the use of computational models may be of benefit in an exploratory study aiming to examine the mechanisms that contribute to clot formation. Various computational models have been developed in effort to elucidate features of aneurysm thrombosis [9]–[13]. Even though they have been developed with different goals in mind, they all make a contribution to the effort of elucidating aneurysm thrombosis. Some of these models have focused on aortic aneurysm thrombosis while others have aimed to understand cerebral aneurysm thrombosis. A distinction is made between these pathologies as it is thought that different mechanisms contribute to thrombus development in the two contexts. In this paper, we use a previously developed computational model to explore clotting patterns that emerge for different mechanical and biochemical inputs [13]. The study aims to examine how these different inputs lead to different outcomes, and which of those outcomes correlate with clot patterns observed *in vivo*.

## 2 METHODS

Two main tasks are described in the methodology of this work. The first pertains to the creation of a suitable, idealised, cerebral aneurysm geometry for examining the features of interest. The second describes the computational model used to simulate the clotting process. Both of these are detailed in the paragraphs that follow. A section detailing the variation in the models is included at the end of the methods section.

### 2.1 Idealised cerebral aneurysm geometry and meshing

An idealised aneurysm geometry was adapted from one described in a paper by Mulder et al [14]. The main motivation for using an idealised geometry in this study was to avoid obtaining results which would be unique to a specific aneurysm case only. Given that the work was carried out in an attempt to derive general principles and observations, an “idealised” aneurysm was deemed most suitable, while bearing in mind that there is a fairly broad range of aneurysm shapes and sizes. The geometry was created as a surface in CFD-GEOM (ESI Group, Paris, France), the geometry creation tool of the CFD-ACE+ Multiphysics Package (ESI Group, Paris, France), and can be seen in Figure 1. The geometry consists of the parent vessel with an inlet and an outlet, and a spherical cerebral aneurysm that is attached to the vessel. The neck of the aneurysm is located at the intersection between the parent vessel and the sphere. This surface was than exported as an STL file to CFD-VisCART (ESI Group, Par-

is, France), where a non-conforming, Cartesian mesh was created. In addition, boundary regions were defined in this step.

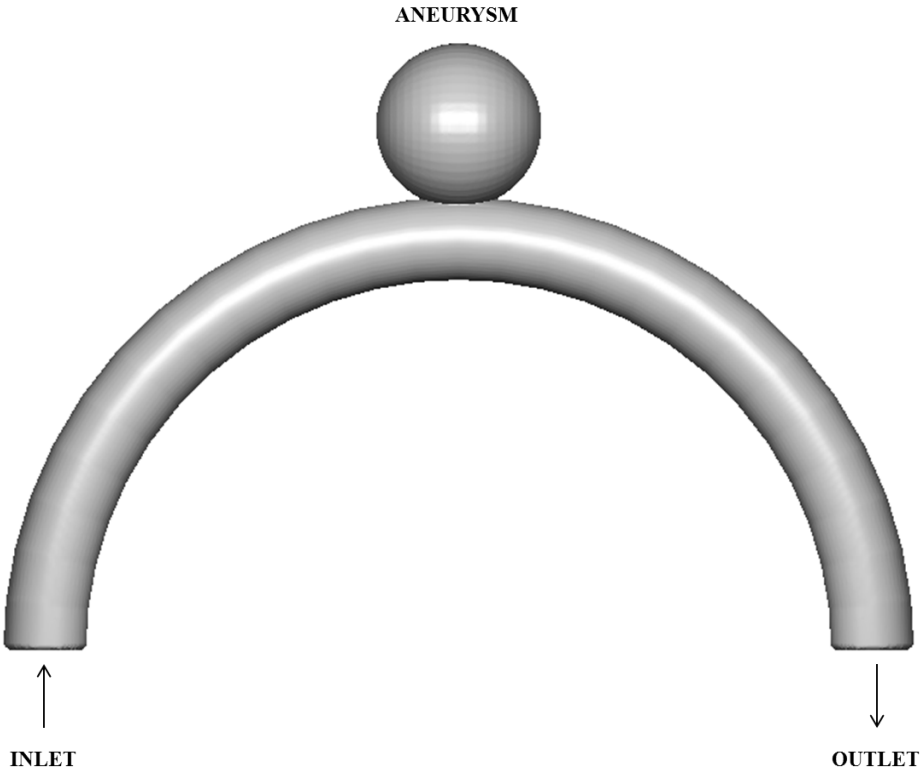


Figure 1: Idealised aneurysm geometry adapted from Mulder et al [14].

## 2.2 Integrated computational model

An integrated computational model capable of accounting for flow, transport of coagulation proteins, reactions between these proteins, the surface of the growing clot and the different properties of the clot region was used. This model consists of four main subsystems, namely flow, porosity and permeability, biochemistry, and level set, which were coupled to ensure that the results of the different systems had bearing on each other. The systems are described in the paragraphs that follow but greater detail can be found in the original paper [13].

The flow submodule describes the flow of blood through the parent vessel and the aneurysm, and accounts for the transport of the coagulation proteins. The continuity and momentum equations are given by (1) and (2), respectively.

$$\frac{\partial \rho}{\partial t} + \nabla(\rho \boldsymbol{U}) = 0 \tag{1}$$

$$\rho \frac{\partial \boldsymbol{U}}{\partial t} + \rho \boldsymbol{U}.\nabla \boldsymbol{U} + \nabla P = \mu \nabla^2 \boldsymbol{U} \tag{2}$$

Where, $\rho$ is density, $t$ is time, $\boldsymbol{U}$ is the velocity vector, $P$ is pressure and $\mu$ is dynamic viscosity. The transport equation which accounts for the transport of the different coagulation proteins is given by (3).

$$\frac{\partial C_j}{\partial t} + \boldsymbol{U}\nabla C_j = \nabla\left(\Gamma_j \nabla C_j\right) + S_j \tag{3}$$

Where, $C_j$ is the concentration of a specific protein, $\Gamma_j$ is the diffusivity of that protein, and $S_j$ is the source of that protein. The diffusivity was adjusted in the clot region to account for the porosity of that region.

In the model, the clot region assumed different porosity and permeability values to the rest of the fluid region. This made it possible for the growing clot to have an impact on the flow region, and vice versa. Using values taken from Diamond and Anand, computational cells which fell within the clot region assumed porosity and permeability values of $\varepsilon = 0.75$ and $\kappa = 1.0\times10^{-12}m^2$, respectively [15].

The biochemistry submodule accounts for the reactions that take place during the coagulation process, and the subsequent changes in the species' concentrations as a result. The coagulation process was described using equations derived by Wagenvoord et al [16]. These were adapted from a six-reaction system to a four-reaction system, as seen in Table 1. Reactions were described using Michaelis-Menten kinetics, or first order kinetics. A stiff equation solver developed by Hairer and Wanner was coded into the user-defined subroutines using FORTRAN [17].

| Step | Reaction Pathway | Forward Reaction Pathway ($nM^{-1}s^{-1}$) | kcat ($s^{-1}$) | kM (nM) |
|---|---|---|---|---|
| 1 | X + TF → Xa-Va + TF | | 5.00E-02 | 1.00E+02 |
| 2 | PT + Xa-Va → TH+ Xa-Va | | 8.00E-02 | 1.00E+03 |
| 3 | V + TH → Xa-Va + TH | | 2.50E+01 | 5.50E+04 |
| 4 | TH + AT → INACT | 5.00E-06 | | |

Table 1: Reaction constants for the adapted Wagenvoord model [16].

The level set submodule enables the tracking of the clot surface [18]. This is important as the careful distinction of the clot region from the rest of the fluid region enables the assignment of different properties to the different regions. The level set equation is given by (4).

$$\phi_t + V_n.|\nabla\phi| = 0 \tag{4}$$

Where $\phi_t$ is the partial derivative of the signed distance function with respect to time, $V_n$ is the propagation velocity of the clot surface and $\phi$ is the signed distance function. In this study, $V_n$ varies and details of the variation are given in the next section.

## 2.3 Variation in models

In order to explore the contributions of mechanics and biochemistry to clot development, it is necessary that input factors be varied. The first set of variations relates to the initiation of clot growth, while the second focuses on clot propagation. In the tables that follow, the propagation velocity column details the equation used for Vn for that case. Initial [TF] gives the starting tissue factor concentration applied at the initiating surface. For cases where tissue factor expression is dependent on a threshold strain rate value, the critical strain rate gives the value above or below which tissue factor is expressed on the initiating surface. Finally, the initiation surface specifies the surface on which tissue factor is expressed for clot initiation. The experiments detailed in Tables 2 and 3 are designed to explore clot initiation. Table 2 illustrates the variation in shear rate threshold for tissue factor expression. Below or above a

certain threshold, tissue factor is expressed, enabling clot initiation. Table 3 details the variations in initial tissue factor concentration required to initiate clotting in the aneurysm sac.

| Case | Propagation velocity ($m.s^{-1}$) | Initial [TF] (M) | Critical Strain Rate ($s^{-1}$) | Initiation surface |
|---|---|---|---|---|
| SR100 | $V_n = a[TH]$ | 1.00E-17 | 100 | SR<100$s^{-1}$ on wall |
| SR500L | $V_n = a[TH]$ | 1.00E-17 | 500 | SR<500$s^{-1}$ on wall |
| SR500G | $V_n = a[TH]$ | 1.00E-17 | 500 | SR>500$s^{-1}$ on wall |
| SR800 | $V_n = a[TH]$ | 1.00E-17 | 800 | SR>800$s^{-1}$ on wall |

Table 2: Parameters for different critical strain rate models.

| Case | Propagation velocity ($m.s^{-1}$) | Initial [TF] (M) | Critical Strain Rate ($s^{-1}$) | Initiation surface |
|---|---|---|---|---|
| TFconc18 | $V_n = a[TH]$ | 1.00E-18 | N/A | Entire wall |
| TFconc17 | $V_n = a[TH]$ | 1.00E-17 | N/A | Entire wall |
| TFconc15 | $V_n = a[TH]$ | 1.00E-15 | N/A | Entire wall |
| TFconc12 | $V_n = a[TH]$ | 1.00E-12 | N/A | Entire wall |

Table 3: Parameters for models with different initial tissue factor concentrations.

For clot propagation, the propagation velocity, $V_n$, bears relation to the quantity of interest as described in Tables 4 and 5. In Table 4, relationships with mechanical variables are detailed while in Table 5, relationships with biochemical factors are shown.

| Case | Propagation velocity ($m.s^{-1}$) | Initial [TF] (M) | Critical Strain Rate ($s^{-1}$) | Initiation surface |
|---|---|---|---|---|
| Mech_Const | $V_n = a$ | N/A | N/A | Entire wall |
| Mech_SRDir | $V_n = a \times StrainRate$ | N/A | N/A | Entire wall |
| Mech_SRInv | $V_n = a/StrainRate$ | N/A | N/A | Entire wall |

Table 4: Parameters for models linking propagation velocity to mechanical variables.

| Case | Propagation velocity ($m.s^{-1}$) | Initial [TF] (M) | Critical Strain Rate ($s^{-1}$) | Initiation surface |
|---|---|---|---|---|
| Bio_ThromDir | $V_n = a[TH]$ | 1.00E-12 | N/A | Entire wall |
| Bio_ThromInv | $V_n = a/[TH]$ | 1.00E-12 | N/A | Entire wall |
| Bio_ExtTenase | $V_n = a[XaVa\_E]$ | 1.00E-12 | N/A | Entire wall |
| Bio_TotTenase | $V_n = a[XaVa\_T]$ | 1.00E-12 | N/A | Entire wall |

Table 5: Parameters for models linking propagation velocity to biochemical species concentrations

## 3 RESULTS

A comparison of clotting outcomes for different models is presented in this section. Distinction is made between results for clot initiation and those for progression.

### 3.1 Clot initiation

Clot growth for different strain rate thresholds is illustrated in Figure 2. For this model, a strain rate of 500$s^{-1}$ is the defining value above which no clot development is observed. Below this value, clot development is uniform, regardless of the threshold value.

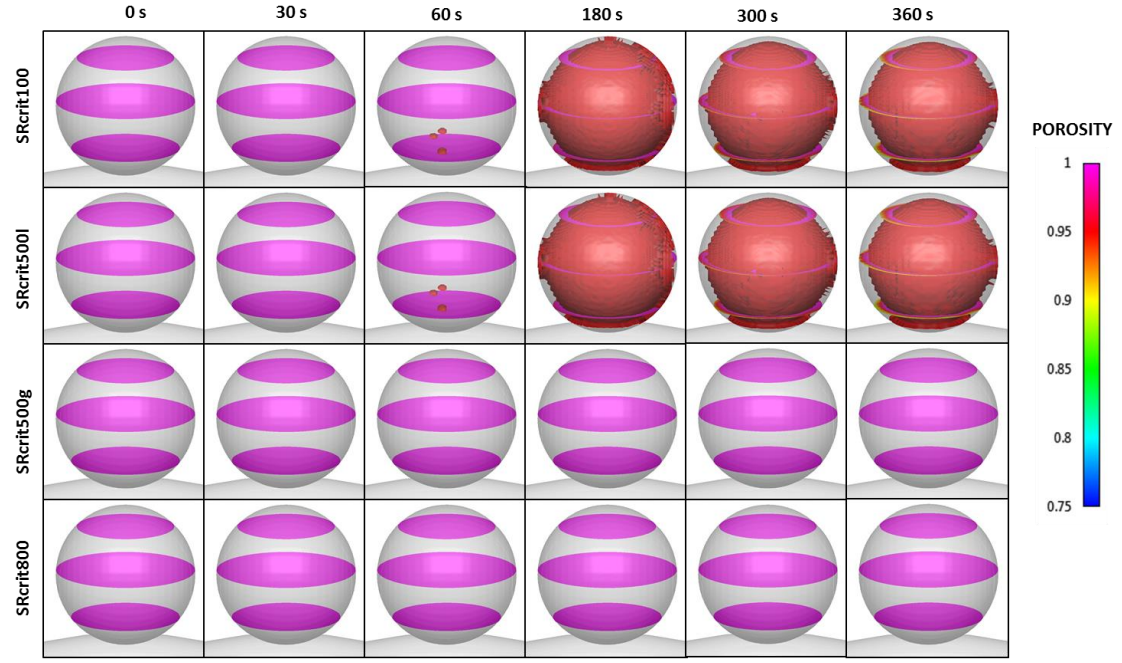


Figure 2: Clot growth for different initiation strain rate thresholds. Below or above a given threshold on the aneurysm wall, tissue factor is expressed.

The clotting process can be initiated for different tissue factor concentrations as seen in Figure 3. An increase in tissue factor concentration results in faster clot growth, however the difference in clot growth becomes less significant as concentration increases.

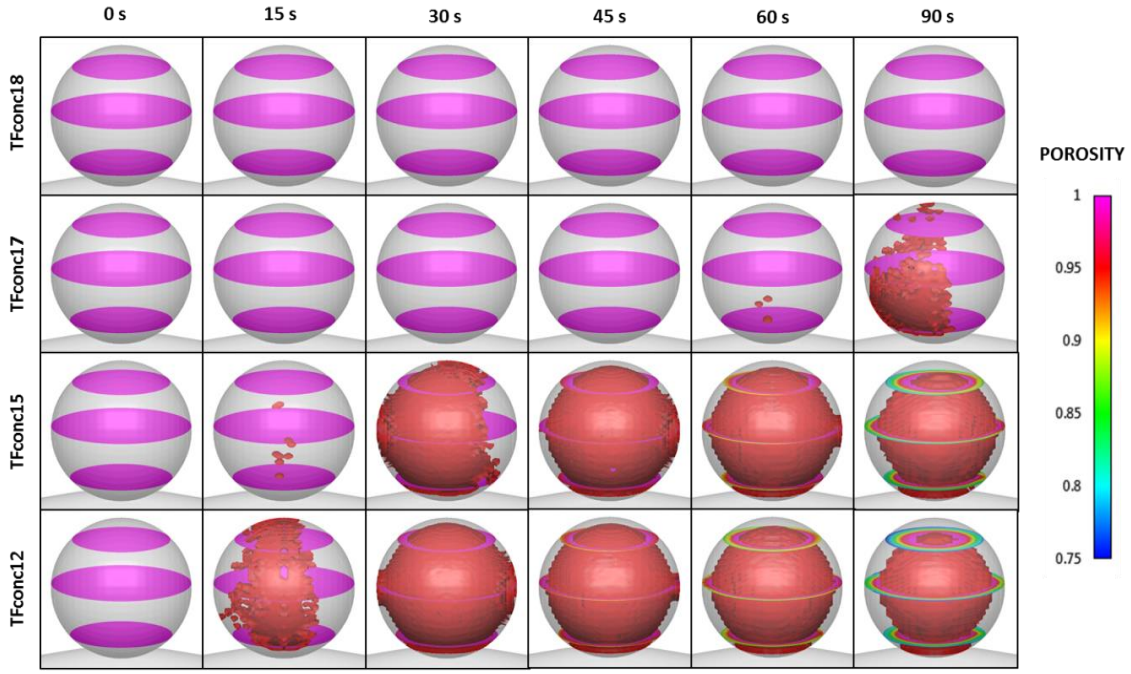


Figure 3: Clot growth for different starting concentrations of tissue factor.

### 3.2 Clot progression

Clot propagation velocity can be linked to mechanical variables as illustrated in Figure 4. Linking direct strain rate results in very rapid occlusion of the aneurysm sac, but also results in clot growth in the aneurysm sac. An inverse relationship between propagation velocity and strain rate results in an asymmetrical clot in the aneurysm sac.

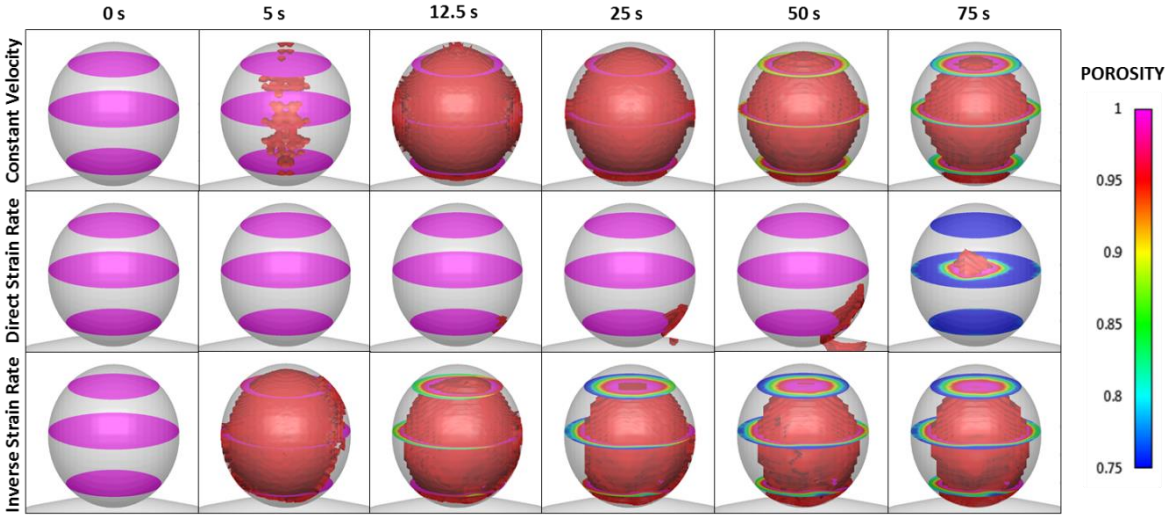


Figure 4: Clot growth when propagation velocity is linked to different mechanical variables.

When clot propagation velocity is linked to the concentrations of different biochemical species, the result produced, regardless of the species, is fairly uniform. This is illustrated in Figure 5. A time lag can be seen when comparing the results of thrombin and tenase because thrombin can only form once tenase is formed.

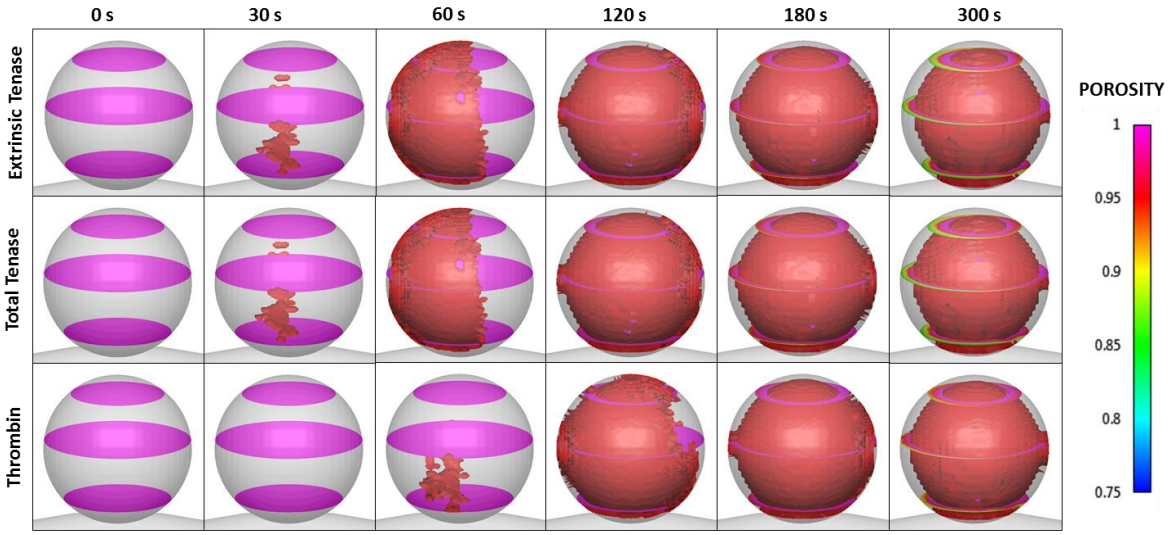


Figure 5: Clot growth when propagation velocity is linked to the concentrations of different biochemical species.

## 4 DISCUSSION

Clot initiation can be regulated either by controlling the initial tissue factor concentration or by regulating the strain rate at which tissue factor is expressed. From the results presented

in the previous section, it seems that the strain rate threshold has a much greater impact on whether or not a region is able to support clot growth. For strain rates greater than $500s^{-1}$, no clotting is observed. Savage et al found that clot deposition governed by fibrin typically occurred at lower shear rates [19]. In this study, the clotting process is governed by the biochemical cascade which eventually results in the formation of fibrin. The results observed therefore support the assertion made by Savage et al. The initial tissue factor concentration seems to have a greater impact on the rate at which the clot subsequently develops, but does not seem to influence whether or not a clot forms. Other studies have also observed that clot initiation in aneurysms seems to correlate with regions of low strain rate [11], [12].

Once clot growth has been initiated, propagation of the clot seems to be governed more by biochemical variables. The results presented show a large variation in clotting outcome for different mechanical variables. The type of clot growth into the parent vessel as illustrated by the direct strain rate model is something that is rarely observed *in vivo*. On the contrary, the biochemical models illustrate typical clotting patterns [1]. The formation and consumption of specific biochemical species in specific places has a significant impact on the stability of the clot [20]. From their studies, Panteleev et al found that extrinsic tenase played a key role in earlier clot propagation, while intrinsic tenase was more instrumental in advanced clot propagation [21]. Thrombin is known to play a key role in thrombus development as it has the ability to activate platelets and amplify its own production [22], [23].

## 5 CONCLUSION

Mechanical and biochemical factors contribute to clot initiation and propagation in cerebral aneurysms. From this exploratory qualitative study, it seems that clot initiation is more closely linked to mechanical factors, while propagation is more dependent on biochemical influences. More work would need to be conducted to verify these observations and to examine the combined effect of mechanical and biochemical factors in both clot initiation and propagation.

## REFERENCES


[1] M. T. Lawton, A. Quiones-Hinojosa, E. F. Chang, and T. Yu, "Thrombotic Intracranial Aneurysms: Classification Scheme and Management Strategies in 68 Patients," *Neurosurgery*, vol. 56, no. 3, pp. 441–454, Mar. 2005.

[2] L. Roccatagliata, P. Guédin, S. Condette-Auliac, S. Gaillard, F. Colas, A. Boulin, A. Wang, S. Guieu, and G. Rodesch, "Partially thrombosed intracranial aneurysms: symptoms, evolution, and therapeutic management.," *Acta Neurochir. (Wien).*, vol. 152, no. 12, pp. 2133–42, Dec. 2010.

[3] J. De Vries, J. Boogaarts, A. Van Norden, and A. K. Wakhloo, "New generation of Flow Diverter (surpass) for unruptured intracranial aneurysms: a prospective single-center study in 37 patients.," *Stroke.*, vol. 44, no. 6, pp. 1567–77, Jun. 2013.

[4] J. E. Cohen, E. Itshayek, E. Yitshayek, J. M. Gomori, S. Grigoriadis, G. Raphaeli, S. Spektor, and G. Rajz, "Spontaneous thrombosis of cerebral aneurysms presenting with ischemic stroke.," *J. Neurol. Sci.*, vol. 254, no. 1–2, pp. 95–8, Mar. 2007.

[5] J.-N. Vallée, L. Pierot, A. Bonafé, F. Turjman, P. Flandroy, J. Berge, G. Rodesch, and S. Bracard, "Endovascular treatment of intracranial wide-necked aneurysms using

three-dimensional coils: predictors of immediate anatomic and clinical results.," *AJNR. Am. J. Neuroradiol.*, vol. 25, no. 2, pp. 298–306, Feb. 2004.

[6] J. V Byrne, R. Beltechi, J. a Yarnold, J. Birks, and M. Kamran, "Early experience in the treatment of intra-cranial aneurysms by endovascular flow diversion: a multicentre prospective study.," *PLoS One*, vol. 5, no. 9, pp. 1–8, Jan. 2010.

[7] V. M. Gonçalves, N. Cristino, and M. C. Sá, "Case Report Spontaneous Thrombosis in Giant Aneurysm of the Anterior Communicating Artery Complex in Pediatric Age : Five-Year Follow-Up," *HindawiiCase Reports Vasc. Med.*, vol. 2014, 2014.

[8] I. R. Whittle, N. W. Dorsch, and M. Besser, "Spontaneous thrombosis in giant intracranial aneurysms.," *J. Neurol. Neurosurg. Psychiatry*, vol. 45, no. 11, pp. 1040–7, Nov. 1982.

[9] P. Di Achille, G. Tellides, C. A. Figueroa, and J. D. Humphrey, "A haemodynamic predictor of intraluminal thrombus formation in abdominal aortic aneurysms," *Proc. R. Soc. London A Math. Phys. Eng. Sci.*, vol. 470, no. 2172, Oct. 2014.

[10] J. Biasetti, P. G. Spazzini, J. Swedenborg, and T. C. Gasser, "An integrated fluid-chemical model toward modeling the formation of intra-luminal thrombus in abdominal aortic aneurysms," *Front. Physiol.*, vol. 3, no. July, pp. 1–16, Jan. 2012.

[11] V. L. Rayz, L. Boussel, L. Ge, J. R. Leach, a J. Martin, M. T. Lawton, C. McCulloch, and D. Saloner, "Flow residence time and regions of intraluminal thrombus deposition in intracranial aneurysms," *Ann. Biomed. Eng.*, vol. 38, no. 10, pp. 3058–69, Oct. 2010.

[12] R. Ouared, B. Chopard, B. Stahl, D. a. Rüfenacht, H. Yilmaz, and G. Courbebaisse, "Thrombosis modeling in intracranial aneurysms: a lattice Boltzmann numerical algorithm," *Comput. Phys. Commun.*, vol. 179, no. 1–3, pp. 128–131, Jul. 2008.

[13] M. Ngoepe and Y. Ventikos, "Computational modelling of clot development in patient-specific cerebral aneurysm cases," *J. Thromb. Haemost.*, vol. 14, no. February 2016, pp. 262–272, 2016.

[14] G. Mulder, A. C. B. Bogaerds, P. Rongen, and F. N. Vosse, "On automated analysis of flow patterns in cerebral aneurysms based on vortex identification," *J. Eng. Math.*, vol. 64, no. 4, pp. 391–401, Mar. 2009.

[15] S. L. Diamond and S. Anand, "Inner clot diffusion and permeation during fibrinolysis.," *Biophys. J.*, vol. 65, no. 6, pp. 2622–43, Dec. 1993.

[16] R. Wagenvoord, P. W. Hemker, and H. C. Hemker, "The limits of simulation of the clotting system.," *J. Thromb. Haemost.*, vol. 4, no. 6, pp. 1331–8, Jun. 2006.

[17] E. Hairer and G. Wanner, *Solving ordinary differential equations II. Stiff and differential-algebraic problems*. Springer, 1993.

[18] S. Osher and R. Fedkiw, *Level Set Methods and Dynamic Implicit Surfaces*, 1st ed. New York: Springer, 2003.

[19] B. Savage, E. Saldívar, and Z. M. Ruggeri, "Initiation of platelet adhesion by arrest onto fibrinogen or translocation on von Willebrand factor," *Cell*, vol. 84, no. 2, pp. 289–97, Jan. 1996.

[20] S. Falati, P. Gross, G. Merrill-Skoloff, B. C. Furie, and B. Furie, "Real-time in vivo imaging of platelets, tissue factor and fibrin during arterial thrombus formation in the

mouse.,” *Nat. Med.*, vol. 8, no. 10, pp. 1175–81, Oct. 2002.

[21] M. a Panteleev, M. V Ovanesov, D. a Kireev, A. M. Shibeko, E. I. Sinauridze, N. M. Ananyeva, A. a Butylin, E. L. Saenko, and F. I. Ataullakhanov, “Spatial propagation and localization of blood coagulation are regulated by intrinsic and protein C pathways, respectively,” *Biophys. J.*, vol. 90, no. 5, pp. 1489–500, Mar. 2006.

[22] B. Furie and B. C. Furie, “In vivo thrombus formation,” *J. Thromb. Haemost.*, vol. 5, no. Supplement S1, pp. 12–17, 2007.

[23] M. Hoffman, “A cell-based model of coagulation and the role of factor Vlla,” *Blood Rev.*, vol. 17, pp. S1–S5, 2003.